# PVC/Montmorillonite Nanocomposites Based on a Thermally Stable, Rigid-Rod Aromatic Amine Modifier

**Zhu-Mei Liang, Chao-Ying Wan, Yong Zhang, Ping Wei, Jie Yin**

*Research Institute of Polymer Materials, School of Chemistry and Chemical Technology, State Key Lab of Composite Materials, Shanghai Jiao Tong University, Shanghai 200240, People's Republic of China*

Received 9 July 2003; accepted 18 September 2003

**ABSTRACT:** Two kinds of polyvinyl chloride (PVC)/montmorillonite (MMT) nanocomposites were prepared by the melt intercalation method based on a thermally stable, rigid-rod aromatic amine modifier and a commonly used 1-hexadecylamine. The information on morphological structure of PVC/MMT nanocomposites was obtained using XRD and TEM. The mechanical, thermal, and flame retardant properties of the nanocomposites were characterized by universal tester, DMA, TGA, and cone calorimeter. The degree of degradation of PVC was studied by $^1$H-NMR. MMT treated by the aromatic amine exhibited better dispersibility than that treated by 1-hexadecylamine. The nanocomposites, based on this MMT, consequently exhibited better mechanical, thermal, and flame retardant properties and lower degradation degree than those based on 1-hexadecylamine-treated MMT.© 2004 Wiley Periodicals, Inc. J Appl Polym Sci 92: 567—575, 2004

**Key words:** montmorillonite; nanocomposites; polyvinyl chloride; aromatic amine modifier

## INTRODUCTION

The field of polymer/clay nanocomposites or hybrids has recently received considerable attention.[1–25] Since Toyota Research Center[2,3] first reported on a nylon-6/clay nanocomposite, many polymers have been used to prepare polymer/clay nanocomposites successfully, such as polypropylene,[4–8] polystyrene,[9,10] polyimide,[11–14] epoxy resin,[15,16] polycarbonate,[17] and poly(methyl methacrylate).[18,19] These nanocomposites usually possess improved strength, enhanced modulus, decreased thermal expansion coefficient, increased thermal stability, and reduced gas permeability compared to the pure polymers or conventional composites, due to the nanoscale dispersion of clay in polymer matrix, high aspect ratio of clay platelets, and interfacial interaction between clay and polymers.

Polyvinyl chloride (PVC) is one of the most important thermoplastics owing to its wide applications and low cost, and it has been studied and used widely in industrial fields for many years. However, due to its inherent disadvantages, such as low thermal stability and brittleness, PVC and its composites are subject to some limitations in certain applications.[20] Preparing PVC/clay nanocomposite may be one of the effective ways to improve material performance, but few studies have been performed so far in comparison with other polymer matrices. Wang et al.[21] prepared largely intercalated PVC/montmorillonite (MMT) nanocomposites, and they studied the thermal and mechanical properties of the nanocomposites in the presence and in the absence of dioctyl phthalate (DOP). The studies mainly discussed the effect of DOP on the structure and thermal stability of the PVC/organic MMT nanocomposites, and they found that organic MMT played an important role in inducing the degradation of PVC. Still some problems regarding PVC/MMT nanocomposites, such as the degradation mechanism have not drawn much attention.

Before preparation of polymer/MMT nanocomposites, modification is generally required through an ion exchange reaction between organic cations and inorganic cations to render hydrophilic MMT more organophilic and to increase interlayer spacing of MMT, aiming to provide a better physical and chemical environment for the polymer. The commonly used organomodification agents are long carbon-chain alkyl amine or ammonium salts. It has been widely accepted that the interlayer spacing of organically modified layered silicates (OLS) depends greatly on the length of the carbon chain.[1] But, in our previous studies, a thermally stable, rigid-rod aromatic amine modifier was synthesized [Scheme 1 (a)] and applied to prepare polyimide/MMT nanocomposites by *in situ* polymerization[22]and melt intercalation method.[23] The organomodified MMT prepared by this new modifier exhibited a high ion-exchange ratio, higher interlayer spacing, and a higher decomposition temperature.

In this paper, we discuss the preparation of PVC/MMT nanocomposites by the melt intercalation method and investigate the influence of the foregoing

*Correspondence to:* J. Yin (jyin@sjtu.edu.cn).

Journal of Applied Polymer Science, Vol. 92, 567—575 (2004)

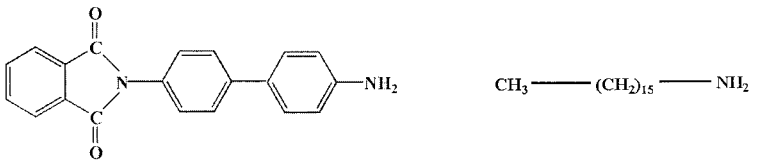


(a) (b)

**Scheme 1** Chemical structure of amine modifiers: (a) OM-*l* and (b) OM-*16C*.

thermally stable, rigid-rod aromatic amine modifier and a commonly used long carbon-chain amine modifier on the mechanical, thermal, and flame retardant properties of nanocomposites. We also examine the influence of these two modifiers on the degradation of PVC.

## EXPERIMENTAL

### Materials

Sodium montmorillonite (Na-MMT) with a cation exchange capacity (CEC) of 100 mEq/100 g was supplied by the Institute of Chemical Metallurgy, Chinese Academy of Sciences. The average particle size is 50 $\mu$m. *N*-[4-(4′-aminophenyl)] phenyl phthalimide (OM-*l*) was synthesized in our lab.[22] 1-Hexadecylamine (OM-*16C*, $C_{16}H_{33}NH_2$, lab reagent) was purchased from Merck Company. Suspension polymerization PVC resin (PVC WS-800, **[GRAPHIC]**) was manufactured by Shanghai Chloro-Alkali Chemical Co., Ltd., China. Various processing additives for PVC, such as organic tin stabilizer (TM181), plasticizer (DOP), and lubricant (paraffin) were industrial-grade products.

### Preparation of organically modified MMT

MMT was organically modified with OM-*l* via ion exchange reaction in water. The mixture of 10.8 g OM-*l*, 1 mL concentrated hydrochloric acid (37%), and 150 mL distilled water was heated to 80°C, and to it was added a dispersion of 25 g Na-MMT in 1,000 mL distilled water. The mixture was stirred vigorously for 1 h at 80°C. The white precipitate was filtered and washed repeatedly with hot water (80°C) to remove the superfluous ammonium salts and make it free from $Cl^-$ and was subsequently collected and vacuum dried at 80°C for 24 h. The preparation of MMT modified with OM-*16C* (MMT-*16C*) followed a procedure similar to that of MMT-*l*.

### Preparation of PVC/MMT nanocomposites

PVC, additives, and various amounts of organomodified MMT were first dry-mixed and then melt-blended in the mixing chamber of a HAAKE Rheometer RC90 at 175°C and a rotor speed of 80 rpm for 8 min. The resultant nanocomposites were then compression-molded into sheets of 1 and 3 mm thickness by a hot press at 175°C and 20 MPa for 10 min, followed by cooling to room temperature at 10 MPa. The sheets were prepared for structure characterization and property measurements (1-mm-thick sheets for tensile strength and dynamic storage modulus tests and 3-mm-thick sheets for impact strength test).

### Characterization

Proton nuclear magnetic resonance ($^1$H-NMR) spectra were recorded after dissolving PVC and PVC/MMT nanocomposites in deuterated tetrahydrofuran (THF-$d_4$), on a Mercury 400MHz NMR spectrometer. A Thermo Jawell Ash IRIS Advantage 1000 inductively coupled plasma spectrometer (ICP) was used to detect the ion exchange ratio of various modifiers.

The change in the basal spacing of MMT was measured on a Rigaku Geiger Flex D/max-RB diffractometer using $CuK_\alpha$ radiation (40 kV, 100 mA,$\lambda$ = 0.154 nm), filtered by Cr. The experiments were performed in a range of $2\theta = 1.0-35°$ with a scan rate of 4°/min. Samples for transmission electron microscopic (TEM) analysis were prepared by placing small strips of sample sheets in epoxy resin and then cut using an ultratome and placed on a 200-mesh copper grid for analysis. The TEM investigation was performed on a JEM-100CXIITEM operating at an acceleration voltage of 100 kV.

The thermal stability of PVC/MMT nanocomposites was measured on a Perkin–Elmer TGA 7 thermal analyzer under $N_2$ flow. The temperature range was 100 to 800°C with a heating rate of 20°C/min.

The dynamic mechanical analysis of the pure PVC and PVC/MMT nanocomposites was performed on a TA 2980 dynamic mechanical analyzer (DMA). The heating rate was 5°C/min.

The stress–strain curves of the pure PVC and the PVC/MMT nanocomposites were recorded on an Instron-4465 universal tester at room temperature with an extension rate of 5 mm/min. Notched Izod impact tests were performed with a Ray Ran Universal Pendulum Impact Tester according to ASTM D256–97 standard, with a hammer speed of 3.5 m/s and pendulum weight of 0.818 kg at room temperature.

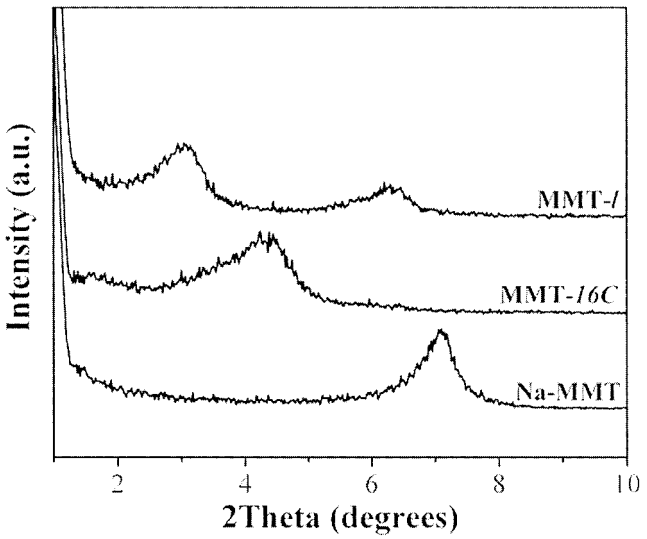


**Figure 1** XRD patterns of Na-MMT, MMT-*l*, and MMT-*16C*.

All cone calorimeter data of PVC and the nanocomposites were obtained using a Stanton Redcroft Cone Calorimeter (Polymer Laboratories, UK) at an incident heat flux of 35 kW/m$^2$.

## RESULTS AND DISCUSSION

### Organomodification of MMT

Figure 1 shows the XRD patterns of Na-MMT, MMT-*l*, and MMT-*16C*. Table I lists the basal spacing of Na-MMT, MMT-*l*, and MMT-*16C* calculated from Bragg's Equation. The interlayer spacing of MMT was obviously increased after the treatment with chloride salt of OM-*l* and OM-*16C* from $d$ = 1.24 nm for pure Na-MMT to $d$ = 2.90 nm for MMT-*l* and $d$ = 2.07 nm for MMT-*16C*. It was found that this basal spacing of MMT-*l* was greater than MMT treated by the commonly used 1-hexadecylamine (MMT-*16C*). This may also suggest that the *d*-value depends not only on the chain length but also on the rigidity of organomodifier molecules.[22] The ICP measurement also revealed a very high ion exchange ratio in the OM-*l*–treated MMT (Table I). All these results suggest that OM-*l* is very effective in modifying MMT.

**TABLE I**
***d*-Value of MMT Modified with Various Organomodifiers and Mean Value of Percent Recovery of Sodium Ions Measured by ICP**

| Sample | 2 $\theta$(°) | $d$(nm) | Sodium ions (wt %) | Ion exchange ratio (%) |
|---|---|---|---|---|
| Na-MMT | 7.12 | 1.24 | 2.3860 | — |
| MMT-*l* | 3.04 | 2.90 | 0.0417 | 98.25 |
| | 6.30 | 002 | peak | |
| MMT-*16C* | 4.26 | 2.07 | 0.0560 | 97.65 |

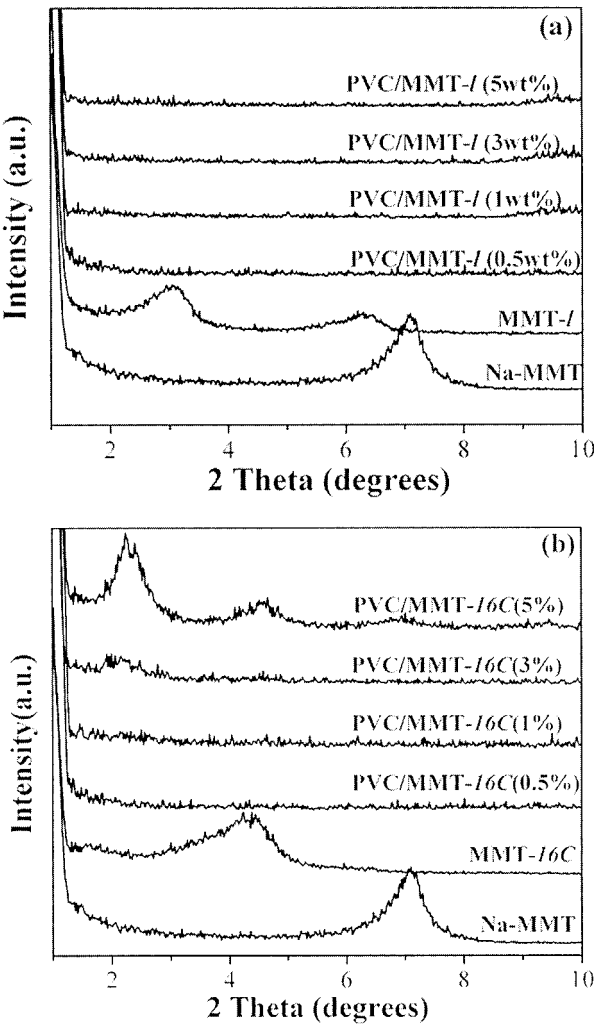


**Figure 2** XRD patterns of (a) PVC/MMT-*l* and (b) PVC/MMT-*16C* nanocomposites with various MMT contents.

### Dispersion of MMT in PVC matrix

Figures 2(a) and (b) show the XRD patterns of Na-MMT, organomodified MMT, the PVC/MMT-*l* and PVC/MMT-*16C* nanocomposites, respectively. Figure 2(a) shows that the diffraction peak of MMT-*l* disappeared completely in the nanocomposites even when the MMT content was up to 5 wt %. This may indicate exfoliated dispersion of MMT-*l* in PVC. As shown in Figure 2(b), when the MMT content was below 1 wt %, the diffraction peak of MMT-*16C* disappeared; when the MMT content was above 3 wt %, the diffraction peak at $2\theta$ = 2.25° ($d$ = 4.36 nm) was still visible; and when the MMT content was 5 wt %, the 001 diffraction peak at $2\theta$ = 2.37 was obvious. The foregoing results indicate that the MMT-*l* layers with higher *d*-values were more favorable to the intercalation of PVC mol-

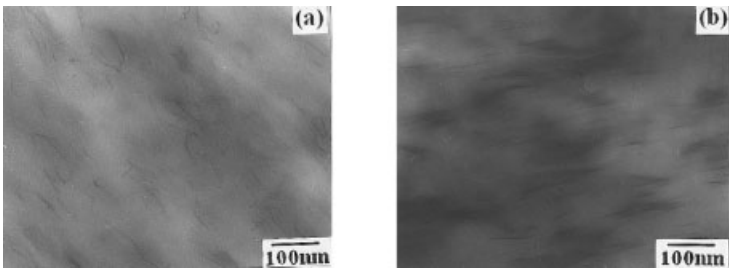


**Figure 3** TEM micrographs of (a) PVC/MMT-*l* and (b) PVC/MMT-*16C* nanocomposites containing 3 wt % MMT.

ecules and the formation of the exfoliation morphology than MMT-*16C*. The dispersion of MMT in the nanocomposites could be further demonstrated by TEM analysis. Figures 3(a) and (b) show the TEM photographs of PVC/MMT-*l* and PVC/MMT-*16C* nanocomposites containing 3 wt % MMT, respectively. In the TEM photograph, the black lines represent the intersection of the MMT layers while the gray part represents the PVC matrix. In Figure 3(a), we show MMT layers dispersed in PVC matrix homogenously and, combined with the XRD results, these results indicate that PVC/MMT-*l* nanocomposite with 3 wt % MMT formed an exfoliation structure. In Figure 3 (b), we show that orientation of MMT layers occurred and they are arranged much more closely, which indicates PVC/MMT-*16C* nanocomposite with 3 wt % MMT formed an intercalation structure. This result is in good agreement with the XRD result.

### Mechanical properties of PVC/MMT nanocomposites

Figure 4(a) shows the effect of MMT content on the Young's modulus of the PVC/MMT nanocomposites. The introduction of a small amount of MMT, which has a higher modulus than the PVC matrix, led to an obvious increase in the moduli of the nanocomposites, increasing from 3.18 GPa for PVC to 5.35 GPa for PVC/MMT-*l* nanocomposite and 5.10 GPa for PVC/MMT-*16C* nanocomposite with 1 wt % MMT. This increase in modulus may be caused by the increase in the number of exfoliated MMT layers at a low MMT content. When the MMT content was further increased, the Young's modulus of the nanocomposites leveled off or decreased slightly. This phenomenon will be discussed later. Moreover, the moduli of PVC/MMT-*l* nanocomposites were higher than those of PVC/MMT-*16C* nanocomposites at the same MMT content. This may be caused by the better dispersion of MMT in the PVC/MMT-*l* nanocomposites at the same MMT content. This result is in good agreement with XRD and TEM results.

Figure 4(b) shows the effect of MMT content on the tensile strength of the PVC/MMT nanocomposites. The introduction of a small amount of MMT led to an

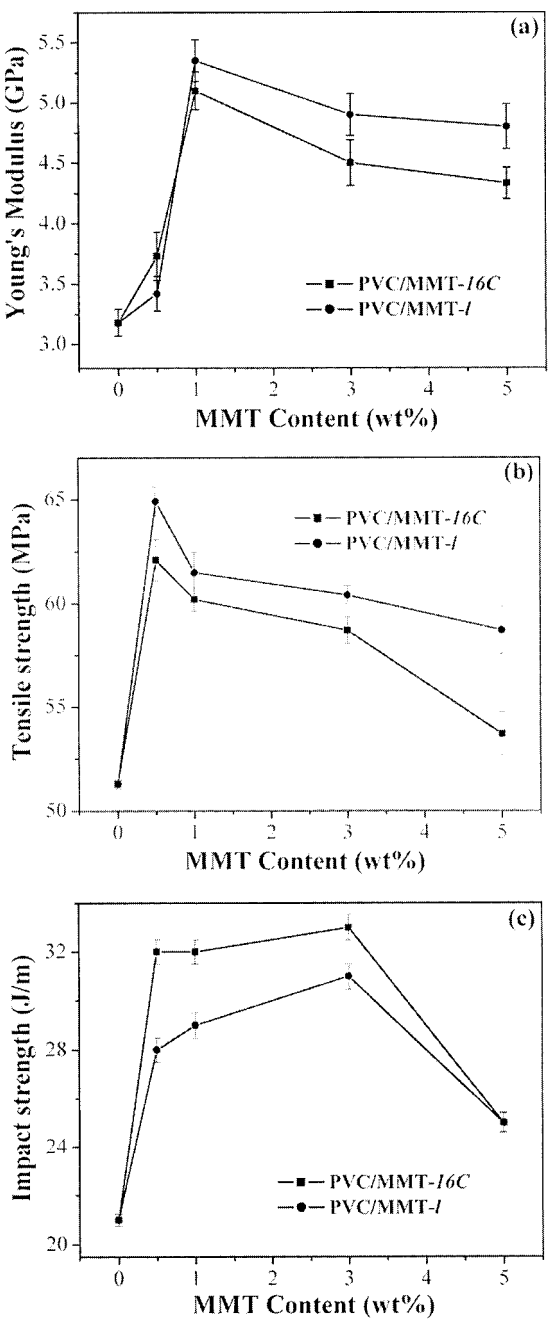


**Figure 4** Relationship between MMT content and (a) Young's modulus, (b) tensile strength, and (c) impact strength of PVC/MMT nanocomposites.

obvious increase in the tensile strength of the nanocomposites. When the MMT content was 0.5 wt %, the tensile strength of PVC/MMT-*l* and PVC/MMT-*16C* nanocomposites was simultaneously increased up to maximum values. The tensile strength was increased from 51.3 MPa for PVC to 64.9 MPa for PVC/MMT-*l* nanocomposite (a 26.5% increase) and 62.1 MPa for PVC/MMT-*16C* nanocomposite (a 21.1% increase). The increase in the tensile strength of the PVC/MMT nanocomposites could be caused by the strong interfacial interaction between MMT and PVC matrix. Furthermore, the tensile strength of PVC/MMT-*l* nanocomposites increased more distinctly than PVC/MMT-*16C* nanocomposites. The molecules of OM-*l* possess stronger polarity than OM-*16C*, which could enhance the interfacial interaction between the layered silicates and PVC matrix. Moreover, from the XRD results, the MMT layers in PVC/MMT-*l* nanocomposites had better dispersibility than in PVC/MMT-*16C* nanocomposites. This may be the reason for the difference in the tensile strength of these two types of PVC/MMT nanocomposites.

The impact strength of PVC and PVC/MMT nanocomposites with various MMT contents is shown in Figure 4(c). The PVC/MMT nanocomposites were toughened by the introduction of MMT. When the MMT content was below 3 wt %, the impact strength was increased with increasing MMT content. The impact strength increased from 21 J/m for PVC to 31 J/m for PVC/MMT-*l* (a 47.6% increase) and to 33 J/m for PVC/MMT-*16C* (a 57.1% increase) nanocomposites containing 3 wt % MMT. Moreover, it was also found that PVC/MMT-*16C* nanocomposites had slightly higher impact strength than PVC/MMT-*l* nanocomposites.

It was found that the tensile strength, impact strength, and Young's modulus were increased as the MMT content was increased to a certain value, and then decreased. But they were higher than those of pure PVC in MMT contents studied. Gilman and coworkers[24] found that the quaternary alkyl ammonium in MMT somehow contributed to the degradation of PS, had a direct negative impact on the flame-retardancy, and could also limit the improvement in other physical properties observed for PS/MMT nanocomposites. For PVC/MMT nanocomposites, the concentration of organomodifier was increased when the MMT content was increased, which might cause the degradation of PVC and the decrease in tensile strength, impact strength, and Young's modulus. This point of view will be discussed later.

The change in the dynamic storage moduli of PVC and PVC/MMT-*l* nanocomposites with temperature is shown in Figure 5(a). The dynamic storage moduli of the nanocomposites were higher than that of PVC and increased with increasing MMT content. Figure 5(b) shows the tanδ curves of PVC and PVC/MMT-*l* nanocomposites with various MMT contents. With the increase of MMT content, the tanδ peak of PVC/MMT-*l* nanocomposites gradually shifted to a slightly higher temperature and became broader in comparison to PVC. This could be also explained by the existence of a strong interaction between MMT and PVC matrix, which limited the movement of the PVC chain. Table II shows the dynamic storage moduli of PVC and PVC/MMT nanocomposites at various temperatures and their glass transition temperatures obtained from tanδ. It was found that the storage moduli of PVC below and above its $T_g$ were increased when a small amount of MMT was introduced.

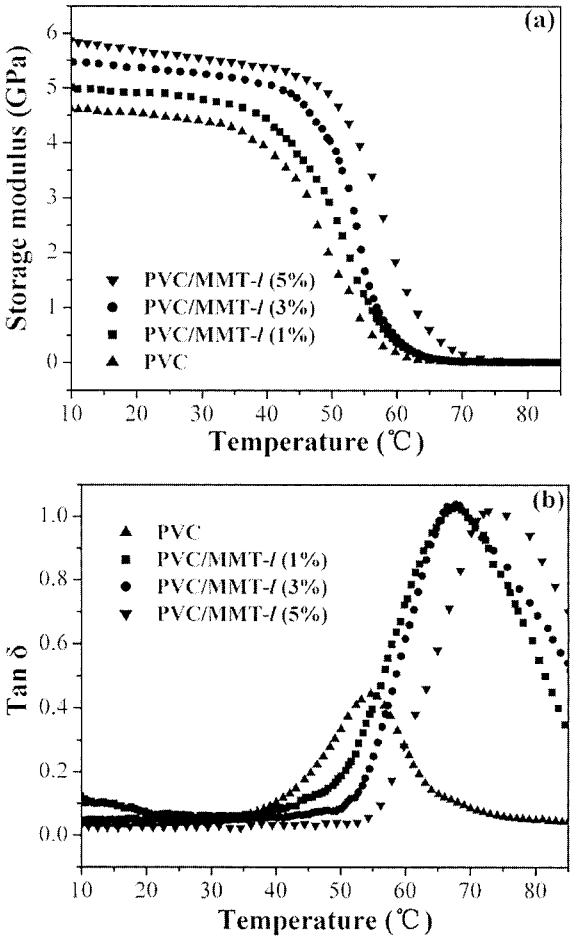


**Figure 5** (a) Storage moduli and (b) tanδ curves of PVC and PVC/MMT-*l* nanocomposites with various MMT contents.

Figure 6 shows the dynamic mechanical analysis (DMA) curves of the PVC/MMT-*l* and PVC/MMT-*16C* nanocomposites containing 5 wt % MMT. It was found that the PVC/MMT-*l* nanocomposite possessed a higher storage modulus and a higher glass transition temperature than the PVC/MMT-*16C* nanocomposite with the same MMT content. This may be attributed to the better dispersion of MMT-*l* in PVC matrix and the stronger interaction between MMT-*l* and PVC matrix than MMT-*16C*.

**TABLE II**
**Dynamic Storage Modulus of PVC and PVC/MMT Nanocomposites and Their Glass Transition Temperatures Obtained from tanδ**

| Sample | Storage modulus (GPa) | | | | Glass transition temperature* (°C) |
|---|---|---|---|---|---|
| | 15°C | 35°C | 55°C | 75°C | |
| PVC | 4.57 | 4.25 | 0.67 | 0.01 | 54.6 |
| PVC/MMT-*l*(1%) | 4.95 | 4.73 | 1.16 | 0.02 | 67.8 |
| PVC/MMT-*l*(3%) | 5.43 | 5.22 | 1.67 | 0.03 | 68.2 |
| PVC/MMT-*l*(5%) | 5.77 | 5.46 | 3.65 | 0.08 | 72.8 |
| PVC/MMT-*16C*(5%) | 5.52 | 4.72 | 0.21 | 0.02 | 59.7 |

* The glass transition temperatures were measured at the peak tops of tanδ.

### Thermal properties of PVC/MMT nanocomposites

The data in Table III show the on-set thermal decomposition temperatures and temperatures at 5 and 10% wt loss of PVC and PVC/MMT nanocomposites in $N_2$ assessed by TGA. They were slightly increased when MMT content was below 1 wt %. The on-set thermal decomposition temperature was increased from 293°C for PVC to 302°C for PVC/MMT-*l* nanocomposite and 297°C for PVC/MMT-*16C* nanocomposite containing 1 wt % MMT. MMT possessed higher thermal stability and its layer structure exhibited a great barrier effect to hinder the evaporation of the small molecules generated in the thermal decomposition to limit the continuous decomposition of the PVC matrix. When the MMT content was increased continuously, the thermal stability of the nanocomposites increased slowly and, when the MMT content was 5 wt %, the on-set decomposition temperature was the same as pure PVC. The reason was that organic amine could induce the degradation of PVC/MMT nanocomposites. PVC/MMT-*l* nanocomposites showed higher thermal stability than PVC/MMT-*16C* nanocomposites, which was attributed to the different degradation degrees of the nanocomposites resulting from the different molecule structures of OM-*l* and OM-*16C*. Detailed reasons will be discussed in the following section.

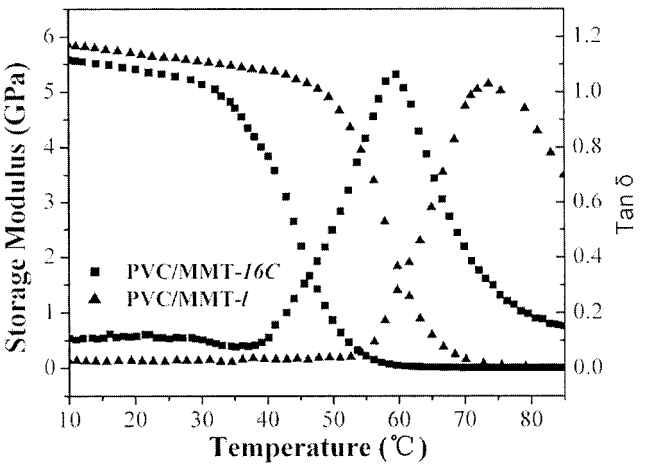


**Figure 6** Storage modulus and tanδ curves of PVC/MMT nanocomposites containing 5 wt % MMT.

### Flame retardant properties of PVC/MMT nanocomposites

Figures 7 and 8 show the heat release rate (HRR) curves and smoke production rate (SPR) curves of PVC and PVC/MMT nanocomposites with 3 wt % MMT content, respectively. Table IV lists the cone calorimeter data of PVC and the nanocomposites. The cone calorimeter study showed that HRR of PVC was much reduced due to the introduction of MMT. For example, when MMT content was only 3 wt %, the peak HRR of PVC/MMT-*l* and PVC/MMT-*16C* was decreased by 48.4 and 42.9%, respectively, and the mean CO and $CO_2$ yields were also reduced. The mean specific extinction area (SEA) was used to estimate the contribution of polymer thermal degradation to smoke and SPR was calculated from production of SEA and mass loss rate. The SEA decreased with the introduction of MMT and resulted in the decrease of SPR. The above results indicate that the nanocomposites possess high flame retardant properties and a smoke prohibition effect. First, MMT as silicate possesses a flame-retardant property. More importantly, MMT layers have a very large aspect ratio and consequently very good barrier properties. The good dispersion of MMT in PVC ensures the existence of a large number of MMT layers even at a relatively low content. The high content of MMT could inhibit the release of CO and $CO_2$ molecules from the PVC matrix effectively. Moreover, PVC/MMT-*l* possesses better cone calorimeter data than PVC/MMT-*16C*, which may be attributed to the better dispersion of MMT-*l* in PVC matrix than MMT-*16C*.

### Degradation studies of PVC/MMT nanocomposites

PVC, as a very important thermoplastic, still possesses many problems due to its rather low thermal stability. Since this polymer shows poor stability during processing, much research has been directed at under-

**TABLE III**
**On-set Thermal Decomposition Temperatures and 5% and 10% Weight Loss Temperatures of PVC and PVC/MMT Nanocomposites**

| MMT content (wt %) | PVC/MMT-*l* (wt%) | | | | PVC/MMT-*16C*(wt%) |
|---|---|---|---|---|---|
| | 0 | 1 | 3 | 5 | 1 |
| $T_d$ (°C)[a] | 293 | 302 | 296 | 293 | 297 |
| $T_5$ (°C)[b] | 270 | 279 | 274 | 271 | 273 |
| $T_{10}$ (°C)[c] | 288 | 293 | 290 | 290 | 290 |

[a] Thermal decomposition temperature (on-set) from TGA measurement. Scan rate: 20°C/min, $N_2$ protection.
[b] Temperature at 5% weight loss from TGA measurement. Scan rate: 20°C/min, $N_2$ protection.
[c] Temperature at 10% weight loss from TGA measurement. Scan rate: 20°C/min, $N_2$ protection.

standing the degradation behavior and stabilization process.[25,26] The low stability of PVC is related in general to the initiation of dehydrochlorination at defect sites during the degradation process by a zip-elimination mechanism.[27] Recently, some methods have been developed for the determination of the microstructure of degraded PVC such as Laser Raman[28] and FT-IR;[29] NMR[30] is another powerful method to give detailed information in understanding the degradation behavior of PVC. The $^1$H-NMR spectra of methylene and methane regions of PVC, PVC/MMT-*l*, and PVC/MMT-*16C* nanocomposite containing 5 wt % MMT are shown in Figure 9. Rao et al.[31] studied UV degradation of PVC and considered that, in the $^1$H-NMR spectrum of virgin PVC, the peaks in the upfield (1.96–2.30 ppm) correspond to methylene protons ($\beta$-protons) and that at the downfield (4.46 ppm) correspond to methyne protons ($\alpha$-protons). Moreover, the intensity of methylene protons was reduced but the intensity of methyne protons was not much affected upon degradation. Similar results were also observed in our study (Fig. 9). In addition, the integral area ratio of methylene protons to methyne protons reduced from 4.18 for virgin PVC to 4.08 for PVC/MMT-*l* and further to 3.83 for PVC/MMT-*16C* nanocomposite, indicates more methylene protons' participation in the dehydrochlorination process in PVC/MMT-*16C* than in PVC/MMT-*l* nanocomposite. It is widely accepted that the degradation of PVC is in line with the following mechanisms: an ionic reaction mechanism and a free radical reaction mechanism.[32] We thought organic amine induced the degradation of PVC according to the ionic reaction mechanism. The organic ammonium cations play a role of proton as Lewis acid and accelerated chlorine ion separating from the PVC matrix,[33] and then absorb it to form the hydrochloric salt of organic amine, and the salt easily released hydrochloric gas (HCl) at a high process temperature and induced the PVC to self-catalyze degradation. It was concluded that organic amines can catalyze PVC degradation but aromatic amines have less effect on PVC degradation than aliphatic amines, probably because the aromatic amines had an antioxidant effect [34] and reduced the degree of degradation

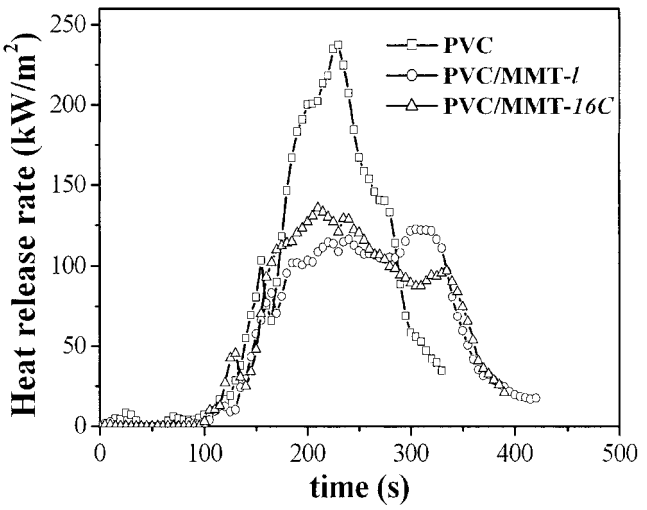


**Figure 7** Heat release rate curves of PVC and PVC/MMT nanocomposites with 3 wt % MMT content.

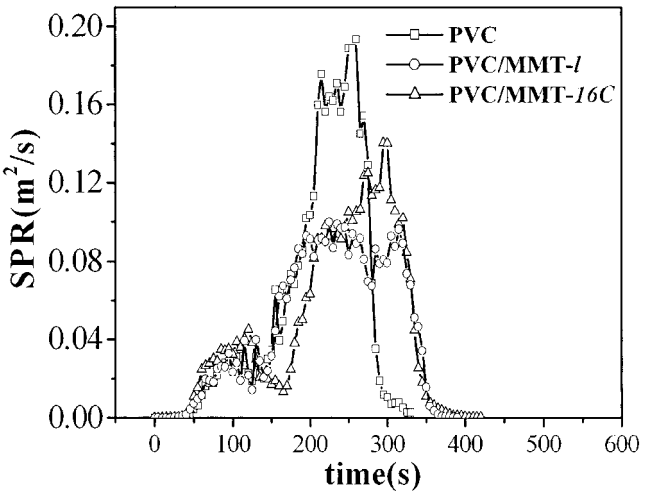


**Figure 8** Smoke production rate curves of PVC and PVC/MMT nanocomposites with 3 wt % MMT content.

**TABLE IV**
**Cone Calorimeter Data of PVC and PVC/MMT Nanocomposites with 3 wt % MMT Content**

| Samples | PVC | PVC/MMT-*l* | PVC/MMT-*16C* |
|---|---|---|---|
| Peak HRR (kW/m$^2$) | 237.6 | 122.6 | 135.6 |
| Average HRR (kW/m$^2$) | 94.7 | 84.3 | 94.3 |
| Mean CO yield (kg/kg) | 0.06 | 0.05 | 0.05 |
| Mean $CO_2$ yield (kg/kg) | 0.86 | 0.64 | 0.64 |
| Mean SEA (m$^2$/kg) | 740.2 | 643 | 643 |
| Time to ignition(s) | 150 | 165 | 145 |

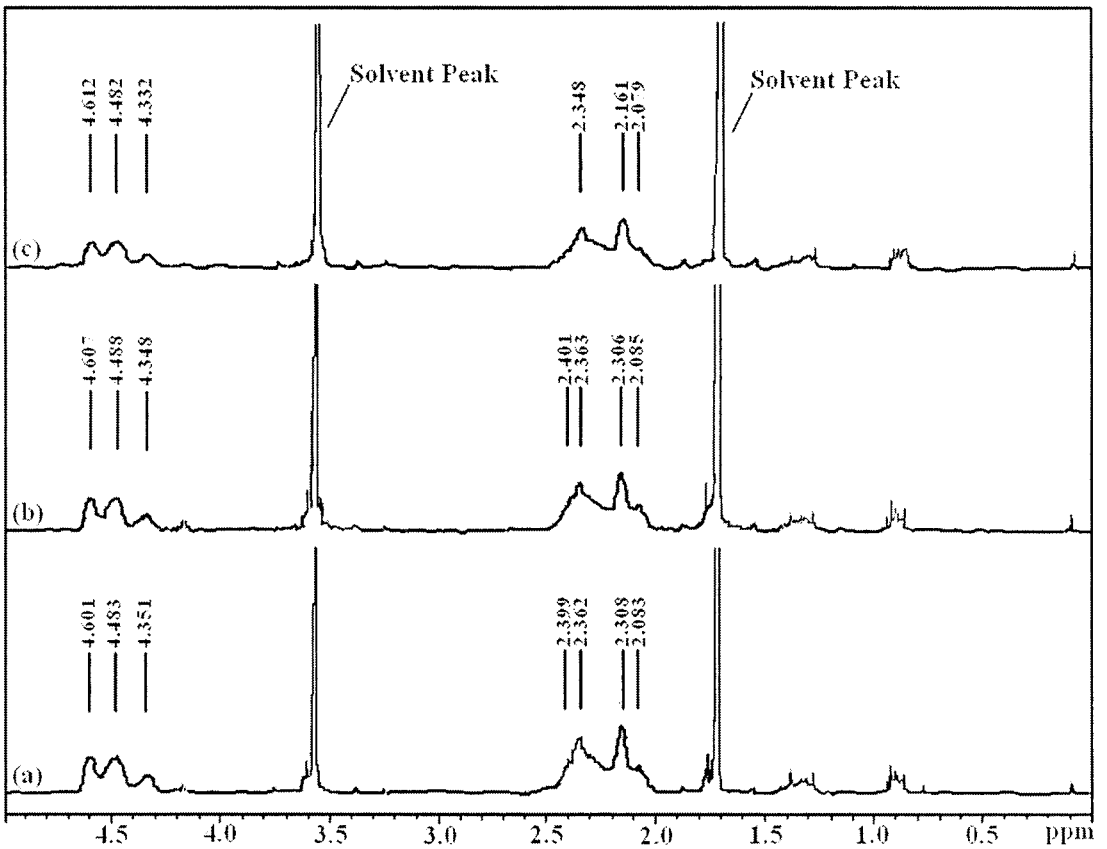


**Figure 9** $^1$H-NMR spectra of (a) PVC, (b) PVC/MMT-*l*, and (c) PVC/MMT-*16C* nanocomposites with 5 wt % MMT content

of PVC/MMT-*l* nanocomposites. Therefore, PVC/MMT-*l* nanocomposites exhibited better mechanical, thermal, and flame-retardant properties than PVC/MMT-*16C* nanocomposites. The degradation mechanism of PVC/MMT nanocomposites is under detailed study.

## CONCLUSION

PVC/MMT nanocomposites have been successfully prepared by the melt intercalation approach. From XRD and TEM results, the MMT layers were basically exfoliated in the PVC/MMT-*l* nanocomposites even when the MMT content was 5 wt % while PVC/MMT-*16C* nanocomposites exhibited intercalation morphology when the MMT content was above 3 wt %. Compared to that of pristine PVC, the stiffness and impact strength of the two kinds of nanocomposites were improved simultaneously within the range of 0.5–3 wt % MMT content. The introduction of a small amount of MMT also led to an improvement in thermal stability and a slight increase in glass transition temperature. PVC/MMT-*l* nanocomposites exhibited better mechanical, thermal, and flame-retardant properties than PVC/MMT-*16C* nanocomposites, which can be attributed to the following: (1) the better dispersion of MMT-*l* in PVC matrix and the stronger interaction between MMT-*l* and PVC matrix than MMT-*16C* and (2) the smaller degree of degradation of PVC/MMT-*l* nanocomposites than PVC/MMT-*16C* nanocomposites.

The authors thank the Ministry of Education of China (Kuashiji Scholars' Project) and Science and Technology Commission of Shanghai Municipal Government (Nano-Project 0214NM019) for their financial support.

## References

1. Giannelis, E. P.; Krishnamoorti, R.; Manias, E. Adv Polym Sci 1999, 138, 107.
2. Kojima, Y.; Usuki, A.; Kawasumi, M.; Okada, A.; Kurauchi, T.; Kamigaito, O. J Polym Sci Part A: Polym Chem 1993, 31, 983.
3. Kojima, Y.; Usuki, A.; Kawasumi, M.; Okada, A.; Kurauchi, T.; Kamigaito, O. J Polym Sci Part A: Polym Chem 1993; 31, 1755.
4. Hasegawa, N.; Kawasumi, M.; Kato, M.; Usuki, A.; Okada, A. J Appl Polym Sci 1998, 67, 87.
5. Kurokawa, Y.; Yasuda, H.; Oya, A. J Mater Sci Lett 1996, 15, 1481.
6. Kawasumi, M.; Hasegawa, N.; Kato, M.; Usuki, A.; Okada, A. Macromolecules 1997, 30, 6333.
7. Zhang, Q.; Fu, Q.; Jiang, L. X.; Lei, Y. Polym Int 2000, 49, 1561.
8. Sun, T.; Garces, J. M. Adv Mater 2002, 14, 128.
9. Doh, J. G; Cho, I. Polym Bull 1998, 41, 511.

10. Zhu, J; Morgan, A. B.; Lamelas, F. J.; Wilkie, C. A. Chem Mater 2001, 13, 3774.
11. Agag, T.; Koga, T.; Takeichi, T. Polymer 2001, 42, 3399.
12. Chang, J. H.; Park, K. M. Polym Eng Sci 2001, 41, 2226.
13. Chin, I. J.; Thurn-Albrecht, T.; Kim, H. C.; Russell, T. P.; Wang, J. Polymer 2001, 42, 5947.
14. Yano, K.; Usuki, A.; Okada, A.; Kurauchi, T.; Kamigaito, O. J Polym Sci Part A: Polym Chem 1993, 31, 2493.
15. Yano, K.; Usuki, A.; Okada, A. J Polym Sci Part A: Polym Chem 1997, 35, 2289.
16. Salahuddin, N.; Moet, A.; Hiltner, A.; Baer, E. Eur Polym Mater 2002, 38, 1477.
17. Huang, X. Y.; Lewis, S.; Brittain, W. J. Macromolecules 2000, 33, 2000.
18. Lee, D. C.; Jang, L. W. J Appl Polym Sci 1996, 61, 1117.
19. Chen, H.; Yao, K.; Tai, J. J Appl Polym Sci 1999, 73, 425.
20. Dietrich, B. J. Vinyl & Addit Tech 2001, 4, 168.
21. Wang, D. Y.; Parlow, D.; Yao, Q.; Wilkie, C. A. J Vinyl & Addit Tech 2001, 7, 203.
22. Liang, Z. M.; Yin, J; Xu, H. J. Polymer 2003, 44, 1391.
23. Liang, Z. M.; Yin, J. J Appl Polym Sci, to appear.
24. Gilman, J. W.; Jackson, C. L.; Morgan, A. B.; Harris, R. H.; Manias, E.; Giannelis, E. P.; Wuthenow, M.; Hilton, D.; Phillips, S. Chem Mater 2000, 12, 1866.
25. Geddes, W. C. Rubber, Chem Technol 1967, 40, 177.
26. Ivan, B.; Kelan, T.; Tudos, F. Degradation and Stabilization of Polymers; Elsevier: Amsterdam, 1989; p. 483.
27. Abbas, K. B.; Laurence, R. L. J Polym Sci Part A: Polym Chem 1975, 13, 1889.
28. Kip, B. J.; Aaken, S. M.; Meier, R. J.; Williams, K. P. J.; Gerrand, D. L. Macromolecules 1992, 25, 4290.
29. Ivan, B.; Kennedy, J. P.; Kelen, T.; Tudos, F. J Macromol Sci Chem 1982, A17, 1033.
30. Starnes, W. H.; Schilling, F. C.; Plitz, I. M.; Cais, R. E.; Freed, J. D.; Hartless, R. L.; Bovey, F. A. Macromolecules 1983, 16, 790.
31. Rao, P. V. C.; Kaushik, V. K.; Bhardwaj, I. S. Eur Polym Mater 1995, 31, 341.
32. Zhao, J. S.; Fu, Z. M. Process and Application 2001, 6, 30.
33. Zheng, Z. Plastics 1999, 28, 8.
34. An, Y. J Technique Exchange 2001, 6, 276.